© 2021. Published by The Company of Biologists Ltd | Journal of Experimental Biology (2021) 224, jeb240705. doi:10.1242/jeb.240705

RESEARCH ARTICLE

Na^+/H^+ exchangers differentially contribute to midgut fluid sodium and proton concentration in the sea urchin larva

Inga Petersen*, William W. J. Chang and Marian Y. Hu*

ABSTRACT

Regulation of ionic composition and pH is a requisite of all digestive systems in the animal kingdom. Larval stages of the marine superphylum Ambulacraria, including echinoderms and hemichordates, were demonstrated to have highly alkaline conditions in their midgut with the underlying epithelial transport mechanisms being largely unknown. Using ion-selective microelectrodes, the present study demonstrated that pluteus larvae of the purple sea urchin have highly alkaline pH (pH ∼9) and low $[Na^+]$ (∼120 mmol l^{-1}) in their midgut fluids, compared with the ionic composition of the surrounding seawater. We pharmacologically investigated the role of Na^+/H^+ exchangers (NHE) in intracellular pH regulation and midgut proton and sodium maintenance using the NHE inhibitor 5-(*n*-ethyl-*n*-isopropyl)amiloride (EIPA). Basolateral EIPA application decreased midgut pH while luminal application via micro-injections increased midgut $[Na^+]$, without affecting pH. Immunohistochemical analysis demonstrated a luminal localization of NHE-2 (SpSlc9a2) in the midgut epithelium. Specific knockdown of *spslc9a2* using Vivo-Morpholinos led to an increase in midgut $[Na^+]$ without affecting pH. Acute acidification experiments in combination with quantitative PCR analysis and measurements of midgut pH and $[Na^+]$ identified two other NHE isoforms, Spslc9a7 and SpSlc9a8, which potentially contribute to the regulation of $[Na^+]$ and pH in midgut fluids. This work provides new insights into ion regulatory mechanisms in the midgut epithelium of sea urchin larvae. The involvement of NHEs in regulating pH and Na^+ balance in midgut fluids shows conserved features of insect and vertebrate digestive systems and may contribute to the ability of sea urchin larvae to cope with changes in seawater pH.

KEY WORDS: Acid–base regulation, Alkaline midgut, Ion-selective microelectrodes, NHE, Ocean acidification, Sodium/hydrogen exchanger

INTRODUCTION

In contrast to the acidic gastric conditions found in most vertebrates, larval stages of many hemichordate and echinoderm species have highly alkaline conditions in their digestive system, with pH values ranging from pH 8.5 to 10.5 (Stumpp et al., 2015; Hu et al., 2017). Highly alkaline conditions are well described in the gut of lepidopteran and dipteran larvae as well as in some termite species (Brune and Kühl, 1996; Boudko et al., 2001a). In insects, these alkaline conditions are believed to be favorable for the digestion of a plant- and lignocellulose-rich diet (Boudko et al., 2001a,b; Brune and Kühl, 1996) and may serve as the first line of immunity against ingested pathogens (Clark et al., 1999). Also, in the sea urchin larva, highly alkaline conditions of the midgut are involved in the breakdown of microalgae and serve as an important mechanism to protect against ingested pathogens (Schwenzfeier et al., 2011; Stumpp et al., 2013, 2020). In contrast to vertebrate and insect models, the ectoderm of the sea urchin larva is permeable for molecules up to 4 kDa (Stumpp et al., 2012). Consequently, the ion composition of the extracellular matrix (ECM) resembles the ion composition of the surrounding seawater and the cells of the midgut epithelium are directly exposed to pH and ionic changes of the environment. Acidification experiments demonstrated that the midgut epithelium has high capacities to maintain midgut fluid pH under a wide range of seawater pH conditions (Lee et al., 2019). However, chronic CO_2-induced acidification down to pH 7.4 directly translated into a small decrease of 0.3 to 0.5 pH units in midgut pH, leading to lower digestion efficiencies due to a shift in the pH optimum for major digestive proteases (Stumpp et al., 2013). Additionally, a previous study demonstrated that strict regulation of highly alkaline midgut conditions (pH 10.5) leads to a high sensitivity of hemichordate larvae to CO_2-induced seawater acidification (Hu et al., 2017).

These studies suggested that energy allocations to the maintenance of a proton gradient up to three orders of magnitude may represent a key trait determining the sensitivity of marine larvae to reductions in environmental pH. Accordingly, the existence and ability to defend midgut pH against large proton gradients across the midgut epithelium indicates the presence of well-developed ion-transporting properties in the larval midgut (Stumpp et al., 2013). Ultrastructural and molecular analyses suggested the presence of at least two different cell types in the midgut epithelium of the sea urchin larva. One cell type is clustered around the area of the cardiac sphincter and seems to be responsible for mediating digestive processes, seen in high expression levels of homologues to mammalian pancreatic genes (Perillo et al., 2016). The second cell type is distributed across the whole midgut epithelium and is rich in mitochondria and vesicles at the basal region of the cells (Burke, 1981). Immunohistological analysis demonstrated Na^+/K^+-ATPase-rich cells scattered over the gut epithelium in sea urchin larva (Stumpp et al., 2013), suggesting that this type of cell is relevant for trans-epithelial ion transport. The recent cell model for pH and ion regulation additionally includes the V^+-type ATPases (VHA) and secondary active sodium/hydrogen exchangers (NHEs) (Stumpp et al., 2015). Ocean acidification experiments in combination with expression analyses demonstrated an upregulation of *NHE-2* (*spslc9a2*) under chronic hypercapnic conditions. This observation has been interpreted as a compensatory mechanism to defend midgut pH against environmental acidification (Stumpp et al., 2012). Pharmacological studies in combination with immunohistological investigations of NHEs suggest an important role for these transporters in larval midgut pH regulation (Stumpp et al., 2015). The ubiquitous

Institute of Physiology, Christian-Albrechts University of Kiel, Hermann-Rodewaldstraße 5, 24118 Kiel, Germany.

*Authors for correspondence (i.petersen@physiologie.uni-kiel.de; m.hu@physiologie.uni-kiel.de)

I.P., 0000-0002-4986-5238

Received 13 November 2020; Accepted 24 February 2021

Journal of Experimental Biology (2021) 224, jeb240705. doi:10.1242/jeb.240705

appearance of Na^+/H^+ exchangers in all organisms and cell types and their primary function for intracellular pH regulation, cell volume and regulation of intracellular sodium concentration by removing protons in exchange for extracellular sodium ions, makes these transporters prime candidates for controlling acid–base conditions in sea urchin larvae (Dibrov and Fliegel, 1998; Saier et al., 1999; Xu et al., 2018). Also, in the intestines of mammals, marine teleosts and insect midguts, alkalization of luminal fluids involves NHEs to control $[Na^+]$ and pH (Onken et al., 2004, 2008; Grosell, 2011). For example, inhibitor studies revealed that in most mammalian species NHE-2 and NHE-3 contribute to neutral $[Na^+]$ absorption in the small intestine and colon coupled to Cl^-/HCO_3^- exchange (Bachmann et al., 2004).

Previous studies addressing the mechanisms of midgut alkalization in the sea urchin larva pointed towards a central role of NHEs in the alkalization processes (Stumpp et al., 2013, 2015; Hu et al., 2017; Stumpp et al., 2020). However, the identification and contribution of specific NHE isoforms to midgut alkalization remained speculative. Here we investigate the role of NHEs in regulating pH and $[Na^+]$ in the alkaline fluids of the larval sea urchin midgut. Using a suite of methods ranging from ion-selective microelectrodes (ISMs) over immunocytochemistry, morpholino knockdown and gene expression analyses, this work provides a detailed analysis of the contribution of NHEs to maintain midgut $[Na^+]$ and pH in the sea urchin larva.

MATERIALS AND METHODS

Experimental animals and larval cultures

Adult purple sea urchins [*Strongylocentrotus purpuratus* (Stimpsin 1857)] were collected on the coast of California (USA) and shipped to the Helmholtz Center of Ocean Research (GEOMAR) in Kiel, Germany. The animals were kept in a re-circulating seawater system within a climate chamber at 11°C and a salinity of 33 practical salinity units (PSU). Spawning of males and females was induced by gentle shaking. Eggs were collected in a 500 ml beaker with filtered natural seawater (FSW). Dry sperm was collected with a pipette from the aboral side and diluted (1:1.000 in FSW) for fertilization. Eggs and sperm were transferred to 500 ml beakers filled with FSW. The fertilized eggs were washed several times with FSW and cultured in 2 liter Erlenmeyer flasks at a density of 25 eggs ml^{-1} at 15°C. For each culture, one male and one female were used. For all experiments, larvae were fed from 3 days post-fertilization (dpf) onward, with *Rhodomonas* sp. at a concentration of 5×10^3 cells ml^{-1}.

Ion-selective microelectrode measurements

In addition to H^+-selective microelectrodes, which were built as previously described (Stumpp et al., 2013, 2015), sodium selective microelectrodes were used to investigate the $[Na^+]$ of midgut fluids in the sea urchin larvae. Sodium-selective microelectrodes were backfilled with 100 mmol l^{-1} NaCl electrolyte and front-loaded with a 150 µm column of the sodium-selective ionophore cocktail II [10% (w/w) sodium ionophore II, 89.5% (v/v) *o*-NPOE, 0.5% (v/v) sodium tetraphenylborate; all chemicals were obtained from Sigma-Aldrich, Germany]. To seal the ISM opening, microelectrodes were additionally front-loaded with PVC (300 µl tetrahydrofuran, 0.01 g PVC) containing 100 µmol l^{-1} of the respective ionophore cocktail.

To ensure a rapid and selective response, the microelectrodes were calibrated by measuring the Nernstian property in a series of FSW adjusted to different pH values (7, 8 and 9; adjusted with NaOH/HCl) or different sodium concentrations including 10 mmol l^{-1}, 50 mmol l^{-1}, 100 mmol l^{-1}, 250 mmol l^{-1}, 300 mmol l^{-1}, 350 mmol l^{-1}, 400 mmol l^{-1}, 450 mmol l^{-1}, 500 mmol l^{-1} and 1 mol l^{-1}. As the calibration for sodium-selective electrodes is not linear, the concentration was natural log-transformed to produce a linear relationship between the measured voltage (mV) and the concentration. An Ag–AgCl (RC2F; WPI, Germany) electrode was used as a reference cell and connected with a 1 mol l^{-1} KCl-containing agar bridge to the perfusion bath.

To exclude measurement artefacts due to an epithelial potential, a microelectrode only filled with 1 mol l^{-1} KCl was used, to confirm the absence of an electrical potential generated by the midgut epithelium as demonstrated earlier (Stumpp et al., 2013).

Intracellular pH measurements using real-time ratiometric fluorimetry and the ammonia pre-pulse technique

To measure the intracellular pH of midgut epithelial cells using the ratiometric, pH-sensitive dye 2′,7′-bis-(2-carboxyethyl)-5-(and-6)-carboxyfluorescein-acetoxymethyl ester (BCECF-AM; Invitrogen, Germany), epidermal cells were removed using the 'bag isolation' method described by Harkey and Whiteley (1980). Briefly, the larvae were carefully washed twice in Mg^{2+}- and Ca^{2+}-free artificial seawater (ASW) and afterwards washed twice in bag isolation medium as previously described (Harkey and Whiteley, 1980), followed by two washing steps in FSW. For dye loading, larvae were incubated in FSW containing 50 µmol l^{-1} BCECF-AM (Sigma, Germany) for 60 min at 15°C.

Intracellular pH (pH_i) regulatory abilities of midgut cells were measured by real-time fluorimetry in combination with the ammonia pre-pulse technique (Stumpp et al., 2012; Hu et al., 2018). Fluorescence intensities were recorded using the Visitron imaging system and an inverted microscope (Observer 1; Zeiss, Germany) equipped with a CCD camera (CoolSNAP HQ2; Photometrics, Tucson, AZ, USA), and analysed using the imaging software Metaflour (Visitron, Puchheim, Germany). The perfusion set-up was equipped with a water jacket cooling system and all measurements were performed at 15°C. The fluorescence ratios were translated to actual pH_i values using ASW solution containing nigericin (Millipore, Darmstadt, Germany) and high potassium (150 mmol l^{-1}) as described previously (Stumpp et al., 2012). For this calibration, different pH steps were used (pH 5.5, 6.5, 7.0, 7.5, 8.0, 9.0) and 9–12 regions of interest were summarized and treated as one replicate (N=1). The ammonia pre-pulse method was used to determine the pH_i regulatory capacities of midgut epithelial cells. Here, the recovery rate (pH_i units min^{-1}) expressed as the slope of the compensation reaction after acidosis was used to determine pH_i regulatory capacities in the presence of different EIPA concentrations. Each measurement was conducted with 4–8 dpf larvae. To generate an inhibition curve and to determine the IC_{50} value, 10, 1, 0.1 and 0.01 µmol l^{-1} EIPA were added during the wash-out period after the ammonia pre-pulse.

Pharmacological characterization of H^+/Na^+ exchange mechanisms in the larval midgut epithelium

Inhibitor incubation

The sea urchin larva has a tight midgut epithelium with very little influx of external fluids during swallowing of food particles (Stumpp et al., 2013), whereas the extracellular matrix that is surrounded by the ectoderm is highly permeable for molecules up to 4 kDa (Stumpp et al., 2012). As EIPA is ∼0.3 kDa in size, we expected the inhibitor to reach the basolateral cell side of the midgut by diffusion through the leaky ectoderm within 45 min (Stumpp et al., 2012). Therefore, inhibitors were applied by bathing larvae in the respective inhibitor solution to access the basolateral side or by direct injection into the midgut to reach luminal membranes. Within the experimentally relevant timeframe (0.5–1 h), we expected EIPA

Journal of Experimental Biology (2021) 224, jeb240705. doi:10.1242/jeb.240705

to affect only the target side via these different application methods for two reasons. First, because of its molecular structure, including charged amino and chloride groups, we expect EIPA to have a low membrane permeability. Second, even if low concentrations of EIPA, may reach the other cell side, the concentration of minimal inhibition will be strongly diluted, probably having no or minimal inhibitory effects. For all incubation experiments, 5–10 larvae (4–8 dpf) were picked from the culture, incubated in the inhibitor (FSW containing the respective EIPA concentration dissolved in DMSO), or control solution (FSW containing 0.1% DMSO) for 90 min at 15°C. After incubation, larvae were transferred to the microscope (Axiovert 135; Zeiss, Germany) equipped with a cooling stage (15°C) and midgut pH or Na^+ concentration were measured using ISMs as previously described (Stumpp et al., 2013, 2015).

Inhibitor injection

To apply the inhibitor to the luminal side, larvae were gastrocopically injected with FSW containing 1 mmol l^{-1} FITC (fluorescein sodium salt; Sigma-Aldrich, Germany) and 0.1% DMSO for controls or FSW containing 1 mmol l^{-1} FITC+10 µmol l^{-1} EIPA for the inhibitor treatment. To avoid unnecessarily long time periods after injection, four to five larvae were taken from the culture and injected under an inverted fluorescence microscope (Axiovert). For the injections, larvae were held in place using a glass pipette (tip diameter 20 µm) to which a slight vacuum was applied. The injection pipette (3–4 µm tip diameter) was carefully inserted through the oesophagus into the stomach using an oil-hydraulic micromanipulator (Nikon; Narishige, Tokyo, Japan), without injuring the gut epithelium. Both pipettes were pulled from glass capillary tubes (GB150F-8P; Science Products, Hofheim, Germany) using a DMZ puller (Zeitz Instruments, Munich, Germany); 0.1 nl was injected into the midgut using a microinjection system (Picospritzer III; Parker, Hollis, NJ, USA). The fluorescence signal of FITC was used to observe successful injection into the larval midgut and to avoid double injections of the four to five larvae. Due to the spherical shape of the larval midgut, we calculated the increase in volume before (V_1) and after injection (V_2) using $V=4/3\times\pi\times r^3$, and used this value to determine the injected volume by subtracting V_2–V_1. For the calculations, pictures of larvae before and after injection were taken and the midgut radius was determined using the free imaging software ImageJ. The average injected volume was calculated to be 0.1 nl and allowed the determination of a final concentration of 5 µmol l^{-1} EIPA in the midgut. To determine the effect of the injection itself, an additional control group with non-injected larvae was measured.

In total, 15–18 larvae from three different fertilizations were measured for each treatment and each larva was treated as one biological replicate.

In addition to the inhibitor experiments, luminal midgut sodium and pH were detected over a time course ranging from 4 to 8 dpf. For every measurement, seven to 20 larvae from at least three different fertilizations were measured.

Immunostaining

For the localization of the sea urchin NHE, SpSlc9a2, a polyclonal antibody raised against a synthetic peptide of the carboxyl-terminal region (CHGHHWIKEKWEEVNHK) of the SpSlc9a2 peptide was used (Hu et al., 2020).

For double staining, the Na^+/K^+-ATPase was localized using a monoclonal antibody designed against the avian alpha subunit of the protein (anti-Na^+/K^+-ATPase alpha 5, Hybridoma Bank, diluted 1:400 in PBST) that has been previously described to recognize the Na^+/K^+-ATPases in sea urchin gut (Stumpp et al., 2013, 2015).

Pluteus larvae were taken from cultures and fixed in 4% (w/v) PFA dissolved in FSW for 15 min at room temperature (RT), carefully rinsed in PBST, and subsequently used for immunofluorescence staining.

To block non-specific binding of the primary antibody, larvae were incubated in PBST containing 5% (v/w) bovine serum albumin (BSA) for 1 h. The samples were incubated with the primary antibodies overnight at 4°C. To remove non-bound antibodies, samples were washed four times in PBST. The secondary antibody (Alexa anti-rabbit Fluro 488 for anti-NHE-2; Santa Cruz Biotechnology; diluted 1:250 in PBST and Alexa anti-mouse Fluro 633 for Na^+/K^+-ATPases; Santa Cruz Biotechnology; diluted 1:250 in PBST) were incubated for 1 h at RT, followed by three washing steps. Samples were analysed with a confocal laser scanning microscope (LSM510; Zeiss).

For negative controls, a peptide compensation assay was performed as previously described (Hu et al., 2018). Therefore, the SpSlc9a2 antibody (diluted 1:150 in PBST) was pre-absorbed with the immunization peptide for 8 h at a peptide concentration of 0.1 mg ml^{-1}. Afterwards, immunofluorescence staining was performed as described previously.

SpSlc9a2 Vivo Morpholino application

Vivo Morpholinos (Vivo MO) are antisense oligonucleotide analogues containing a covalently linked delivery moiety consisting of an octa-guanidine dendrimer, which allows the Vivo MO to enter the cell membrane without further manipulation of the cells, and binds to complementary RNA sequences and blocks the translation of the target gene (Morcos et al., 2008; Ferguson et al., 2014). Here we used a Vivo MO specially designed against the *spslc9a2* gene with the sequence 5′-AGCCCCCAAAAGTCATCTCTGTATT-3′ complementary to the start codon region. The *spslc9a2* Vivo MO was obtained from Gene Tools (Philomath, OR, USA). Previously published studies on sea urchin embryos and pluteus larvae treated with Vivo MOs demonstrated clear knockdown phenotypes in skeleton development and bone morphogenetic protein (BMP) signalling (Heyland et al., 2014; Luo and Su, 2012).

The MO was dissolved in H_2O at a concentration of 0.5 mmol l^{-1} for the stock solution, which was further diluted to 5, 1 and 0.1 µmol l^{-1} as the final working concentrations to which larvae were exposed. For the experiment, 25–30 larvae (4 dpf) were picked from the culture and transferred into 1 ml FSW containing the respective Vivo MO concentration. Negative controls only contained 0.1% H_2O deionized in FSW. Larvae were incubated in these solutions for 24 h and midgut [Na^+] was determined by ISMs. Quantification of SpSlc9a2 protein abundance was determined by immunostaining (performed as described earlier) using the custom-made antibody for SpSlc9a2 (Hu et al., 2020), followed by analysis of the intensity of the fluorescence signal in control larvae and in larvae treated with 1 µmol l^{-1} Vivo MO. Pictures were taken on an inverted fluorescence microscope equipped with a pco.panda sCMOS camera (PCO, Kelheim, Germany) in combination with the VisiScope Life Cell Imaging System (Visitron Systems, Germany) with excitation at 488 nm and emission at 520 nm. To avoid artefactual differences in immunostaining, control larvae and the Vivo MO-treated larvae were stained and treated in parallel using the same solutions and incubation conditions. Pictures were taken in an alternate mode from controls and the Vivo MO-treated larvae using the same exposure times and microscopy settings for every image. The fluorescence intensity analysis was performed using ImageJ. For every larva, 10 regions of interest were set into SpSlc9a2-positive cells of the midgut epithelium and the intensity

was measured and the average value from one larva was used as one replicate.

Acidification experiment

To examine if acidic seawater influenced the pH or [Na^+] of the midgut fluids, pluteus larvae (5 dpf) were exposed to acidified FSW (pH 6.5, buffered with 0.03 mol l^{-1} MES and adjusted with NaOH) for a period of 10 h. Samples were taken directly before the start of the incubation (t_0) and after 1, 2, 4, 6 and 10 h (t_1, t_2, t_4, t_6 and t_{10}). The larval cultures were split directly before the experiment started and half of the culture was incubated in acidic FSW (pH 6.5, low pH treatment) while the other half remained in FSW (pH 8.1, controls). For midgut pH and [Na^+] measurements, larvae were picked from the culture and midgut pH was measured using ISMs. At every time point, two to four larvae from three different cultures (N=3) were measured. To examine if exposure to acidic FSW influenced mRNA expression of putative NHEs in the midgut, quantitative PCR (qPCR) samples were taken from the acidification experiment at the same time points as used for microelectrode measurements and immediately flash-frozen in liquid nitrogen and stored at −80°C.

Reverse transcription and real-time qPCR measurements

For RNA isolation, larvae were homogenized in TriZol (Invitrogen; Waltham, MA, USA) and mRNA was isolated by using Direct-zol RNA MiniPrep Kit (Zymo Research, Freiburg, Germany). Genomic contamination was removed by DNAase I treatment. cDNA was synthesized using a SuperScript IV cDNA synthesis kit (Invitrogen) and expression levels of three different NHE isoforms were quantified by real-time qPCR using LightCycler 480 SYBR Green I Master (Roche, Germany) as previously described (Hu et al., 2018).

Target genes were three members of the Slc9 family (SpSlc9a; NHEs) found in the genome of *S. purpuratus*. The sequences of these genes were obtained from EchinoBase (Cameron et al., 2009; Kudtarkar and Cameron, 2017; http://legacy.echinobase.org/shiny/quantdev/) and the coding regions were used for qPCR primer design (NCBI Primer-Blast; www.ncbi.nlm.nih.gov/tools/primerblast/; Table 1). Primers were tested by PCR to confirm a single amplification product. After calculation of the ΔCt value, expression was normalized to *elf 1a* (elongation factor 1a), which is a suitable reference gene during development and environmental perturbations in the sea urchin larva (Hu et al., 2018, 2020).

Statistical analysis and figures

All experiments and measurements were repeated at least three times. For the statistical analysis and figures, every larva was treated as one biological replicate. All statistical analysis and figures were generated using GraphPad Prism 7. The EIPA incubation experiments and the fluorescence intensity analysis of the Vivo MO were statistically analysed with Student's *t*-test, while the results of EIPA injection experiments, real-time qPCR analyses, *spslc9a2* Vivo MO experiments and the pH_i measurements were analysed using one-way ANOVA followed by Tukey's multiple comparisons post hoc test. Correlation analyses from the acidification experiment were analysed by calculating linear regressions between midgut pH and mRNA expression of *spslc9a2*, *spslc9a7* and *spslc9a8*.

RESULTS

Ontogeny and pharmacological characterization of midgut fluid pH and Na^+ concentrations using ion-selective microelectrodes

Midgut fluid pH and sodium concentration of early pluteus larvae were measured daily from 4 to 8 dpf. The sodium concentration in the midgut was markedly below that of seawater, fluctuating between 68 and 233 mmol l^{-1} with a total average (N=64) of 121±5.47 mmol l^{-1} (Fig. 1A). Accordingly, the ECM contains on average a four times higher Na^+ concentration than fluids of the larval midgut. Highest variability in midgut [Na^+] was detected in 5 and 8 dpf larvae ranging from 70 to 230 mmol l^{-1} with an average [Na^+] of 156 mmol l^{-1}.

Midgut pH during daily measurements showed a slight fluctuation from the lowest pH 8.63 up to pH 9.28 with a total average of all larvae (N=55) at pH 8.79±0.03. In total, the pH measurement had low scattering, and the highest pH values were measured in 5 and 6 dpf larvae (average values: pH 8.90±0.04 and pH 8.99±0.04).

As molecules up to 4 kDa can diffuse through the ECM within several minutes (Stumpp et al., 2012), EIPA incubation was used to address the basolateral side of the larval midgut epithelial cells. The inhibitor incubation led to a partial but significant decrease in midgut pH by 0.13 pH units (P=0.0025) from pH 8.88±0.027 in DMSO-treated control larvae (N=17) to pH 8.75±0.024 in EIPA-treated larvae (N=18).

However, midgut [Na^+] remained unaffected by exposure to 5 µmol l^{-1} EIPA from the basolateral side (Fig. 1B). Control (N=22) and EIPA (N=21)-treated larvae had average sodium concentrations of 107±4.9 and 107±7.5 mmol l^{-1}, respectively.

EIPA injections into the midgut were used to address the function of NHEs on the luminal side of the midgut epithelium. Here, our pH measurements demonstrated no effect at a final concentration of 5 µmol l^{-1} EIPA, directly injected into the larval midgut (Fig. 1C). Larvae injected with EIPA (N=14) had an average pH of 8.91±0.024, while those injected with FSW only containing 0.1% of the vehicle DMSO had an average pH of 8.89±0.029 (N=14). In addition, non-injected controls (N=14) had an average pH of 8.91±0.039 (Fig. 1B). Statistical analysis using one-way ANOVA showed no significant differences between all three groups.

Luminal sodium measurements in EIPA-injected larvae (N=18) revealed a significant increase in [Na^+] (P<0.001, d.f.=46) by 135 mmol l^{-1} compared with larvae injected with the control solution (N=16) only containing 0.1% DMSO and FITC. The average midgut sodium concentration of EIPA-injected larvae was 370±24 mmol l^{-1}, while larvae injected with the control solution had a total average sodium concentration of 235±17 mmol l^{-1}. Despite a significant difference between EIPA- and DMSO-injected larvae, both treatments had a significant (P=0.011) increase in luminal [Na^+] compared with uninjected larvae (N=15) with an average sodium concentration of 166±13 mmol l^{-1}.

Table 1. Primer sequences used for real-time quantitative PCR

Gene name	Symbol	Primer sequence	Amplicon size (bp)	Accession numbers
spslc9a2	*NHE-2*	F5′-AGGAGAAACCTCTGGCAGAGCG-3′ R5′-ACCTGCAATCACCACTACGGGT3′	171	SPU_006845
spslc9a7	*NHE-7*	F5′-TTT GCC GGG ACA GCC ATA TC-3′ R5′-GCA GGT CTT GGA ACA CTG CT-3′	166	SPU_017107
spslc9a8	*NHE-8*	F5′-AGG GTC ACA CCC GGT GAA-3′ R5′-CTG GTA ACT GTT CAT CAG CCG-3′	151	SPU_001356
elongation factor 1a	*ELF1a*	F5′-GAGAGTTTGAGGCTGGTATCT-3′ R5′-GACCTCCCTGACGATTTCTTT-3′	155	NP_001116969

Journal of Experimental Biology (2021) 224, jeb240705. doi:10.1242/jeb.240705

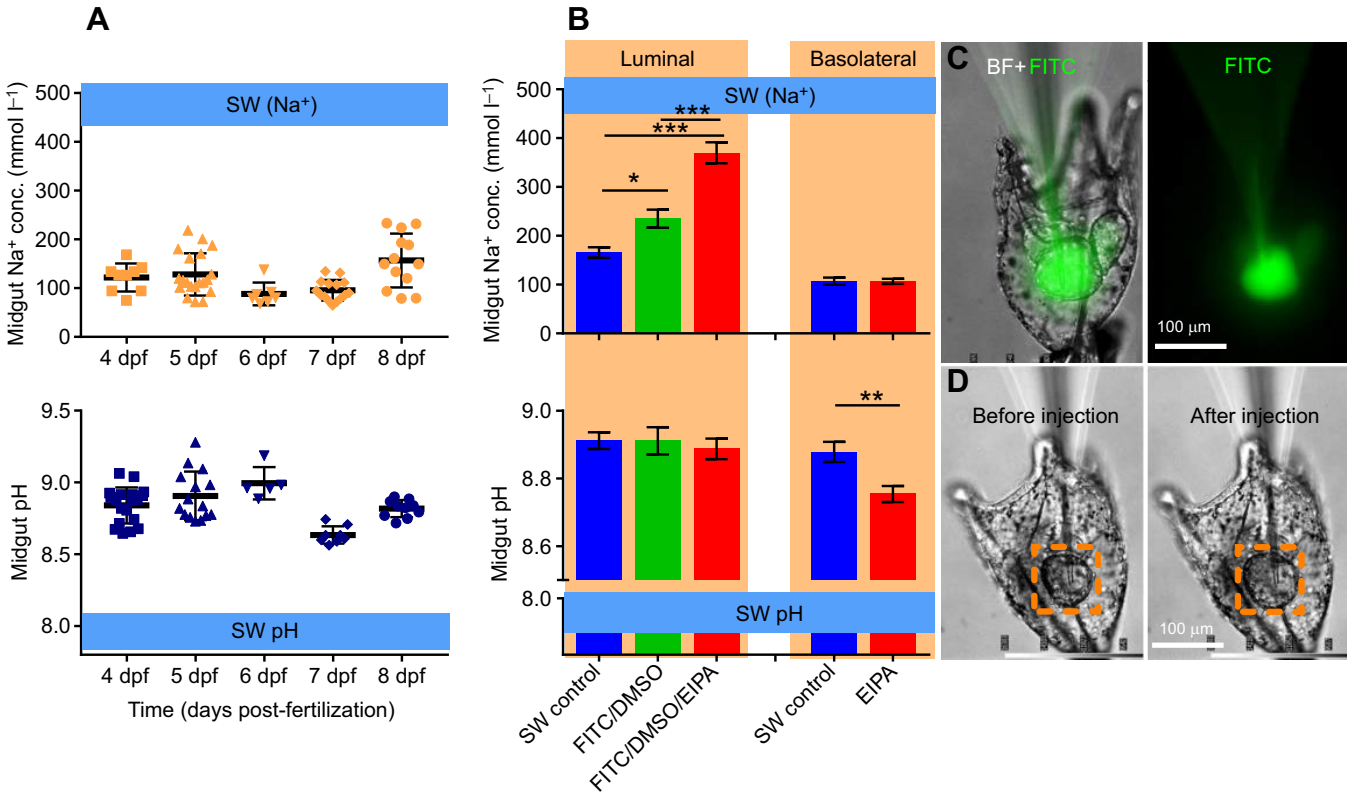

Fig. 1. Pharmacological investigation of midgut [Na^+] and pH using ion-selective microelectrodes. (A) Time course measurement of midgut [Na^+] (upper panel) and pH (lower panel) over development from 4 to 8 dpf. (B) [Na^+] (upper panel) and pH (lower panel) measurements after EIPA injection (5 µmol l^{-1} luminal, pH measurements: seawater (SW) control, FITC/DMSO/EIPA injection, FITC/DMSO injection, *N*=14; [Na^+] measurements: SW control, *N*=15; FITC/DMSO/EIPA injection, *N*=18; FITC/DMSO injection, *N*=16) and EIPA incubation (5 µmol l^{-1} basolateral, pH measurements: controls, *N*=17; EIPA incubation, *N*=18; [Na^+] measurements: controls, *N*=22; EIPA, *N*=21). (C) Example fluorescence image of a larva after luminal injection of the fluorescence dye FITC. BF, bright field. (D) A larva with the inserted injection pipette in the midgut directly before and after injection. The orange dashed rectangle indicates the change in midgut circumference, before and after injection, which was used for the calculation of the final inhibiting concentration. Levels of significance: **P*≤0.011, ***P*≤0.0025, ****P*≤0.001. Values are presented as means±s.e.m.

Effects of EIPA on intracellular pH regulatory capacities of midgut cells

To test the overall contribution of NHEs on pH_i regulatory abilities in midgut epithelial cells, the ammonia pre-pulse technique was used in combination with the pH-sensitive dye BCECF-AM and the NHE specific blocker EIPA. The compensation reaction against the intracellular acidosis was determined by the rate of pH_i recovery expressed as pH_i units min^{-1}. Calibration of BCECF fluorescence ratios to actual pH values resulted in a sigmoidal calibration curve (Fig. 2D). Controls (*N*=15) recovered completely from the pre-pulse-induced acidosis within 20 min at a rate of 0.146±0.003 pH_i units min^{-1}. The ability to recover from the induced acidosis was only partially but significantly (*P*=0.0008) reduced to 0.067±0.007 and 0.047±0.006 pH_i units min^{-1} in cells exposed to 1 µmol l^{-1} (*N*=4) and 10 µmol l^{-1} (*N*=12) EIPA, respectively. Different concentrations of EIPA demonstrated that the midgut epithelial cells reacted sensitively to the NHE inhibitor EIPA in a dose-dependent manner (Fig. 2C) with an IC_{50} of 0.153 µmol l^{-1}. Although the recovery rate was affected by the treatment with EIPA, all cells were able to largely recover from the NH_3/NH_4^+ pre-pulse induced acidosis.

Immunohistological localization of SpSlc9a2, Na^+/K^+-ATPases and mitochondria-rich cells in the larval midgut epithelium

SpSlc9a2 was localized using a custom-made antibody, designed against a synthetic peptide of the *S. purpuratus* SpSlc9a2 protein using confocal microscopy. This antibody was validated in a previous study, demonstrating specific immune reactivity with a 95 kDa protein (Hu et al., 2020). In the pluteus stage, immunofluorescence staining revealed a strong signal in a specific cell type of the midgut epithelium and at higher laser intensities positive immunoreactivity was also detected in primary mesenchyme cells (Fig. 3A–C). Positive immunoreactivity of the SpSlc9a2 antibody was located in luminal membranes of midgut epithelial cells. An overview image of the larval digestive organs (oesophagus, midgut, hindgut) demonstrated a regular distribution of the SpSlc9a2-positive cells scattered over the midgut epithelium with lower signal intensity in the ventral part of the organ (Fig. 3A). A lower density of SpSlc9a2-positive cells was detected close to the cardiac and the pyloric sphincter. The signal for the Na^+/K^+-ATPases was also detected at the luminal side of midgut cells in a similar pattern as observed for SpSlc9a2. Double staining of SpSlc9a2 and Na^+/K^+-ATPases demonstrated a co-localization of the fluorescence signals (Fig. 3C–E). The co-staining of SpSlc9a2 and mitochondria-rich cells using Mitotracker demonstrated a partial co-localization in midgut epithelial cells. Additionally, Mitotracker staining showed a cytosolic signal with different intensities among different cell types of the midgut epithelium (Fig. 3B). Negative controls, using the SpSlc9a2 specific antibody pre-absorbed with the immunization peptide, demonstrated no unspecific binding of the antibodies or auto-fluorescence (Fig. 3E–F).

Journal of Experimental Biology (2021) 224, jeb240705. doi:10.1242/jeb.240705

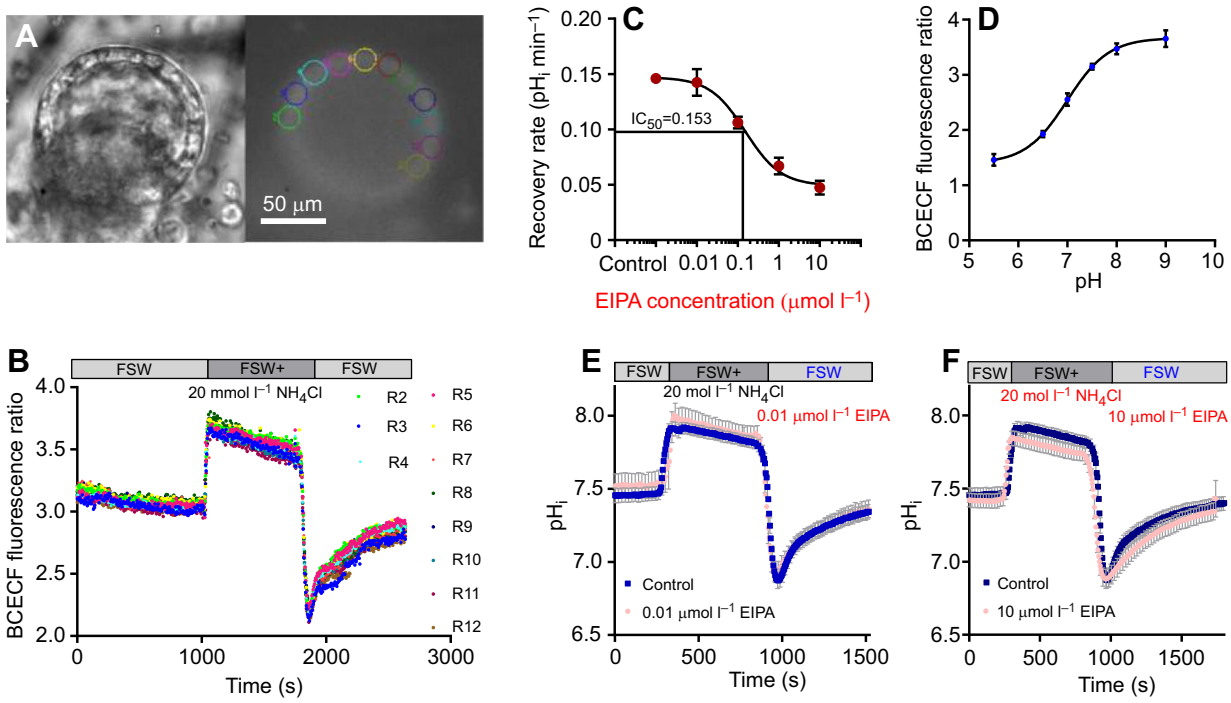

Fig. 2. pH_i regulatory abilities of midgut epithelial cells. (A) Brightfield and fluorescence image (440 nm) of the BCECF loaded midgut epithelium including the regions and original traces (B) during an exemplary measurement under control conditions. The R numbers refer to the regions that were selected and measured in A. (C) Dose–response relationship of midgut epithelial cells during exposure to different EIPA concentrations (*N*=3–12). (D) Average ratios of the measured midgut cells (*N*=4 for every pH step) plotted against different pH values of the nigericin and 150 mmol l^{-1} K^+-containing calibration solution. (E,F) Selected traces from ammonia pulse experiments using different EIPA concentrations [0.01 µmol l^{-1} (*N*=3), 10 µmol l^{-1} (*N*=12), EIPA in red] compared with control cells (blue; *N*=15). Values are presented as means±s.e.m. FSW, filtered natural seawater.

Effects of SpSlc9a2 knockdown on midgut fluid [Na^+] using Vivo Morpholino

Knockdown using Vivo MO specially designed against the coding region of SpSlc9a2 was used to determine the contribution of this protein to the maintenance of [Na^+] in midgut fluids. The ability to maintain midgut [Na^+] was significantly affected by the MO treatment in a dose-dependent manner (Fig. 4; $P<0.0001$). After exposure to 1 µmol l^{-1} SpSlc9a2, MO larvae showed a significant increase in midgut [Na^+] by 97 mmol l^{-1} compared with control larvae that were only exposed to the vehicle. Larvae exposed to a concentration of 5 µmol l^{-1} fully failed to regulate midgut [Na^+] with an average concentration of 428 mmol l^{-1}. However, at the highest MO concentration of 5 µmol l^{-1}, larvae started to have morphological changes including reduced midgut volume and an increased presence of immune cells in the extracellular matrix. Because of these effects of the MO treatment on the overall physiology and morphology, 1 µmol l^{-1} MO-treated larvae, where no visible side-effects were observed, were used to validate the SpSlc9a2 knockdown by immunofluorescence intensities. The quantification revealed a significant decrease in signal intensity of 21.05 arbitrary units (AU) from 100.51±7.98 AU in the SpSlc9a2 morphants to 79.46±5.23 AU in control larvae (control *N*=31, morphants *N*=40; $P=0.027$) (Fig. 4).

Effects of acidified seawater on pH and [Na^+] in midgut fluids and expression of NHE isoforms

To stimulate the midgut pH regulatory machinery, larvae were exposed to acidic seawater (pH 6.5) over a period of 10 h and midgut pH and Na^+ concentration, as well as the expression levels of the three identified Na^+/H^+ exchanger isoforms in the sea urchin larva, were examined.

The acidic seawater treatment did not affect the luminal sodium concentration, with average values of 103.6±3.7 and 103.9±7.6 mmol l^{-1}, in control and low pH-treated larvae, respectively (Fig. 5B). At the beginning of the low pH experiment, larvae had an average midgut pH of 9.13±0.04. Over the 10 h time course, the low pH-treated larvae reduced midgut pH in a biphasic manner and larvae were able to fully restore pH after 10 h of incubation (Fig. 5A). The first drop in midgut pH by 0.26 pH units occurred after 1 h of incubation, followed by a recovery within the next 2 h. The second drop in pH started after 4 h of incubation with the maximum decrease of 0.72 pH units measured after 6 h. Full pH recovery was measured after 10 h.

Real-time qPCR analysis was used to detect changes in the relative expression of *spslc9a2*, *spslc9a7* and *spslc9a8* between control (normal seawater pH 8.1) and larvae exposed to acidic seawater (pH 6.5) over the period of 10 h. qPCR results demonstrated that the luminal located SpSlc9a2 did not respond to the low pH treatment (Fig. 5C). In contrast, *spslc9a7* constantly increased expression levels with a peak after 6 h of low pH exposure ($P=0.045$; Fig. 5C,D). The third NHE isoform, *spslc9a8*, progressively increased expression levels from 0.00141±0.000276 2^−ΔCt to 0.0048±0.001833 2^−ΔCt over the course of the low pH experiment (Fig. 5E). To relate changes in midgut pH to the expression of NHEs, midgut pH values were plotted against the relative expression of the three different NHE isoforms in control and low-pH treated larvae (Fig. 5F–H). Linear regression models demonstrated a significant ($P=0.0208$; Fig. 5G) relationship between midgut pH and the expression levels of *spslca7* in low pH-treated larvae.

DISCUSSION

Marine larval stages of the superphylum Ambulacraria, including echinoderms and hemichordates, were demonstrated to strictly

Journal of Experimental Biology (2021) 224, jeb240705. doi:10.1242/jeb.240705

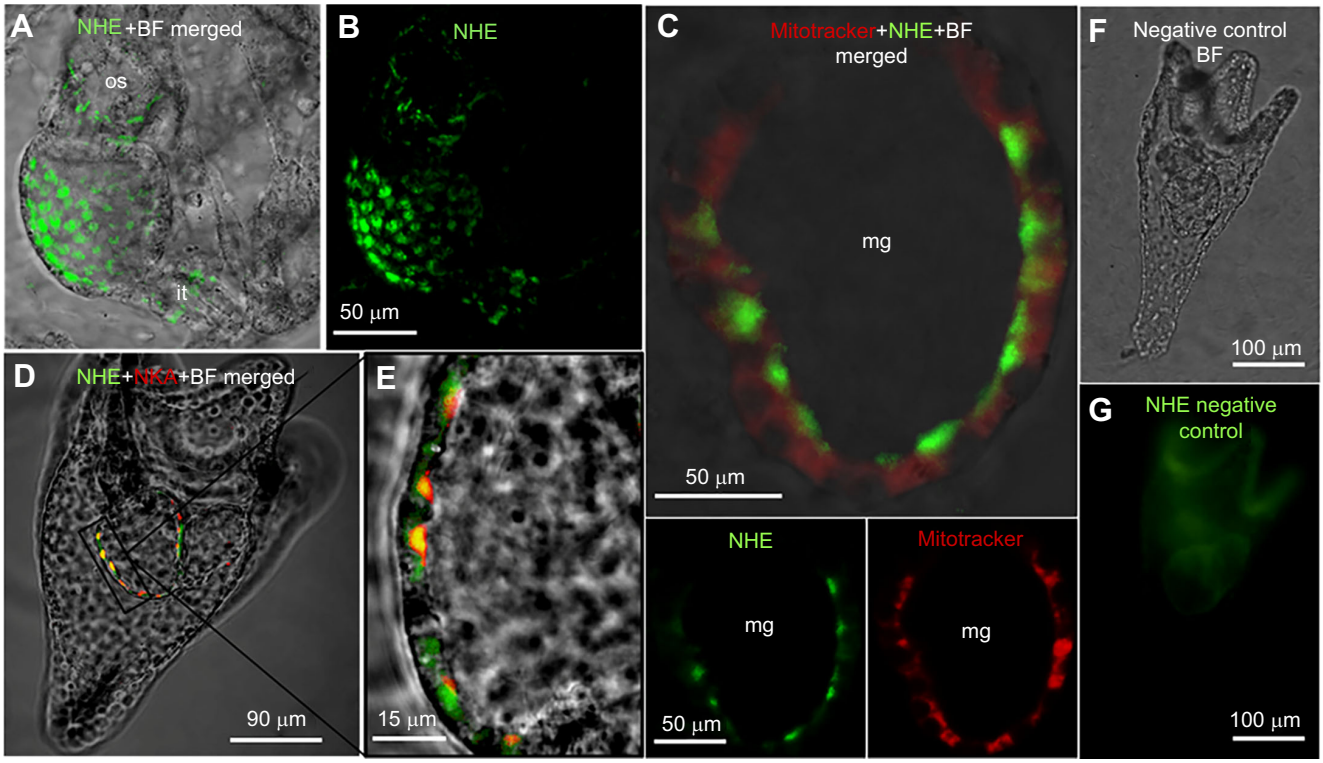

Fig. 3. Immunolocalization of SpSlc9a2 (NHE), Na^+/K^+-ATPase (NKA) and mitochondria-rich cells in the midgut epithelium using laser scanning microscopy. (A,B) Overview of the distribution of SpSlc9a2-positive cells in the midgut epithelium. (C) Co-localization of SpSlc9a2 (green) and mitochondria (Mitotracker, red) in midgut epithelial cells. (D) Co-localization of NKA (red) and NHE (green) in midgut epithelial cells in a 5 dpf larva. (E) High magnification image of the larval midgut showing the signal of NKA and NHE to be largely co-localized in luminal membranes. (F,G) Brightfield and fluorescence image of the SpSlc9a2 antibody pre-absorbed with the immunization peptide. os, oesophagus; mg, midgut; it, intestine.

regulate extracellular pH in their digestive tract (Stumpp et al., 2013, 2015). This acid–base regulatory feature is a key factor associated with energy allocations during exposure to simulated ocean acidification (Stumpp et al., 2013; Hu et al., 2017). On the one hand, a larger fraction of energy is required to maintain pH (Hu et al., 2017) and on the other hand, slight reductions in midgut pH were demonstrated to reduce nutrient uptake by a shift in pH optima of key digestive enzymes (Stumpp et al., 2013). Furthermore, reductions in midgut pH were associated with a higher susceptibility of the sea urchin larva to bacterial infections of the gut (Stumpp et al., 2020). Thus, understanding the mechanistic basis of homeostatic regulation in the larval sea urchin gut will provide important insights into a largely unexplored physiological system and its response to changes in environmental pH. Accordingly, the present work used a suite of methods ranging from the whole organism to the molecular level to address the role of Na^+/H^+ exchangers in regulating pH and $[Na^+]$ in midgut fluids of the sea urchin larva.

Pharmacological and molecular characterization of Na^+/H^+ exchange mechanisms in the regulation of midgut pH and $[Na^+]$

In accordance with previous studies, the present work also confirmed the presence of a highly alkaline environment in the midgut of sea urchin larvae. In addition to this existing knowledge, the present work demonstrated that these organisms also strictly maintain low $[Na^+]$ in their midgut fluids. While midgut pH is typically maintained between pH 8.8 and 9.2, midgut $[Na^+]$ is far below that of seawater (*ca* 450–500 mmol l^{-1}), ranging from 70 to 230 mmol l^{-1}. These observations resemble the situation found in the intestine of marine teleost fish where alkaline conditions together with high rates of bicarbonate secretion support water uptake from the lumen by active NaCl absorption. In marine teleosts, two NHEs (NHE-2 and NHE-3) are localized in luminal membranes of intestinal cells, which are putatively involved in Na^+ resorption from the luminal fluids. Another putative NHE (NHE-1), located at the basolateral side, is thought to be involved in transepithelial Na^+ transport and cytosolic H^+ extrusion (Grosell, 2011). Interestingly, this coordinated interaction between several NHE isoforms located on both sides of the teleost gut epithelium in marine teleosts also seems to be a characteristic of the midgut epithelium in the sea urchin larva. Here the luminal NHE SpSlc9a2, as well as putative NHEs located in basolateral membranes, differentially contribute to the regulation of pH and $[Na^+]$ in midgut fluids. Our experiments demonstrated that basolateral application of EIPA reduces midgut pH but has no effect on midgut $[Na^+]$. In contrast, luminal injection of EIPA led to an increase in midgut $[Na^+]$ levels with no detectable changes in pH. Reaching the basolateral side is possible as large molecules up to 4 kDa can diffuse and distribute within the ECM within 60 min (Stumpp et al., 2012). At the same time, it is unlikely that large amounts of the inhibitor reach the luminal side as swallowing of microalgae is associated with negligible ingestion of external fluids (Stumpp et al., 2013). This is further supported by our observation that midgut pH or $[Na^+]$ showed negligible changes during swallowing, suggesting that no or only very small amounts of water are ingested into the gut. Our results demonstrated that NHEs located on the basolateral side are involved in pH regulatory processes of the midgut, whereas those located in luminal membranes contribute to the maintenance of midgut fluid $[Na^+]$.

Journal of Experimental Biology (2021) 224, jeb240705. doi:10.1242/jeb.240705

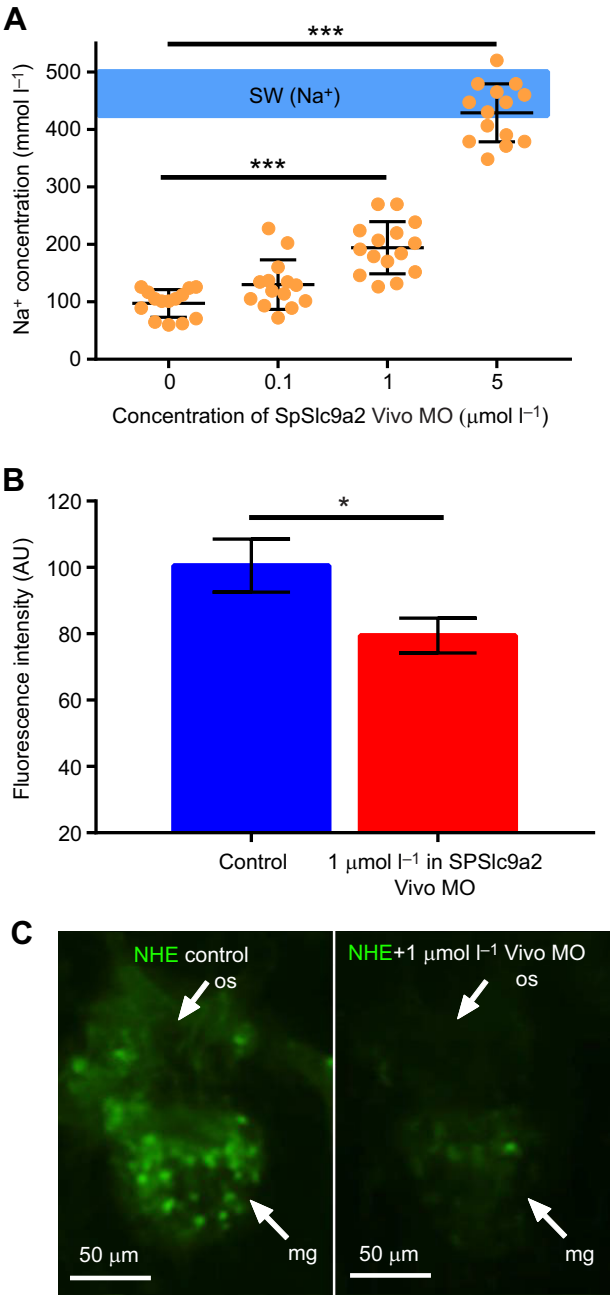

Fig. 4. Effect of *spslc9a2* knockdown on midgut [Na^+]. (A) Midgut [Na^+] in control larvae and in larvae exposed for 24 h to different concentrations of the Vivo Morpholino (Vivo MO; *N*=14–15). (B) Fluorescence intensity (arbitrary units, AU) of SpSlc9a2 immunoreactivity in midgut cells from control (*N*=31) and 1 µmol l^{-1} Vivo MO (*N*=40)-treated larvae. (C) Representative immunostaining of SpSlc9a2 (NHE) in control and 1 µmol l^{-1} Vivo MO-treated larvae.*P<0.05, ***P<0.0001. Values are presented as means±s.e.m. SW, seawater; os, oesophagus; mg, midgut.

Besides the example of the marine teleost gut, an involvement of basolateral NHEs in luminal alkalization has also been suggested in the highly alkaline ventriculus (up to pH 11) of the *Aedes aegypti* mosquito larvae. Pharmacological experiments using amiloride or Na^+-free solutions together with immunocytochemistry suggested an involvement of basolateral NHEs to luminal alkalization (Onken et al., 2004; Pullikuth et al., 2006; Onken et al., 2008). Besides a putative $Na^+/2H^+$ exchanger at the luminal side, the recent cell model includes luminal HCO_3^- secretion via an HCO_3^-/Cl^- exchanger and a $Na^+/2HCO_3^-$ co-transporter, probably supported by basolateral NHEs and V-ATPases (Onken et al., 2004; Pullikuth et al., 2006; Onken et al., 2008). We hypothesize that also in the sea urchin larva basolateral NHE activity acts in concert with luminal HCO_3^- secretion to maintain highly alkaline conditions in the midgut. Besides the sea urchin midgut, there are currently only two other known examples, including the anterior midgut of mosquito larvae and the retinal pigment epithelium of mammals, where the Na^+/K^+-ATPase is localized in luminal membranes (Okami et al., 1990; Patrick et al., 2006; Stumpp et al., 2015). Although it is striking that two of these systems are designed to generate a highly alkaline midgut, its biological significance remains a matter of future work.

Using teleost fish and insect larvae as a guide, we hypothesized that midgut alkalization in the sea urchin larva involves an as yet unidentified HCO_3^- transporter in combination with an intracellular carbonic anhydrase (Fig. 6). Protons generated by intracellular CO_2 hydration can be removed by the basolateral NHEs, and HCO_3^- can be secreted into the lumen to alkalize the larval midgut. This luminal bicarbonate secretion may involve an electrogenic anion exchanger, transporting HCO_3^-/Cl^- in a 2/3:1 stoichiometry as described for the alkaline fish gut (Grosell, 2011). Such a HCO_3^- transport system could explain the near-zero transepithelial potential by using the lumen-positive potential generated by the Na^+/K^+-ATPases and the VHA located in luminal membranes (model; Fig. 6). Although previous studies found no effect of the carbonic anhydrase inhibitor acetazolamide and the anion exchange inhibitor 4,4′-diisothiocyano-2,2′-stilbenedisulfonic acid (DIDS) on midgut alkalization in the sea urchin larva (Stumpp et al., 2015), our experiments demonstrated that complex molecules are not necessarily able to reach the luminal side via bathing of larvae in the inhibitor solution. Inhibitors like DIDS or acetazolamide should be used by direct injection of the inhibitor into the midgut lumen. This would provide important pharmacological evidence about the potential involvement of HCO_3^- transport in the alkalization process, potentially leading to conserved mechanisms of luminal alkalization, as found in the guts of marine teleosts or several insect larvae (Ridgway and Moffett, 1986; Boudko et al., 2001a; del Pilar Corena et al., 2001; del Pilar Corena et al., 2004; Grosell et al., 2005; Grosell, 2011).

The lack of a transepithelial potential in the midgut of the sea urchin larva may also be explained by the presence of an electrogenic $Na^+/2H^+$ antiporter as located in insect epithelia and the distal nephron of humans (Kondapalli et al., 2017; Okech et al., 2008; Chintapalli et al., 2015). Alternatively, cation transport to counter a lumen positive potential may involve a putative K^+/H^+ antiporter with a stoichiometry of $1K^+$:$2H^+$ as proposed in earlier studies using vesicles of highly purified apical membranes of goblet cells for measuring ATP-dependent proton transport and K^+/H^+ antiport (Wieczorek et al., 1991; Azuma et al., 1995). The presence of such an electrogenic cation antiporter at high expression levels would help to explain the near-zero transepithelial potential by counteracting the electrical potential generated by luminal VHA and NKA (Fig. 6). Immunohistological analyses of the sea urchin NHE isoform SpSlc9a2 using a custom-made antibody demonstrated localization of this protein in luminal membranes. Here it is partially co-localized with the Na^+/K^+-ATPase as well as with mitochondria-rich cells. These findings are following previous studies that demonstrated the luminal localization of an NHE isoform using an antibody designed against the teleost NHE-3 (Stumpp et al., 2015). Knockdown of *spslc9a2* resulted in an increased midgut [Na^+] compared with control animals, lending strong evidence for this NHE isoform to be responsible for the regulation of [Na^+] in midgut fluids. The luminal

Journal of Experimental Biology (2021) 224, jeb240705. doi:10.1242/jeb.240705

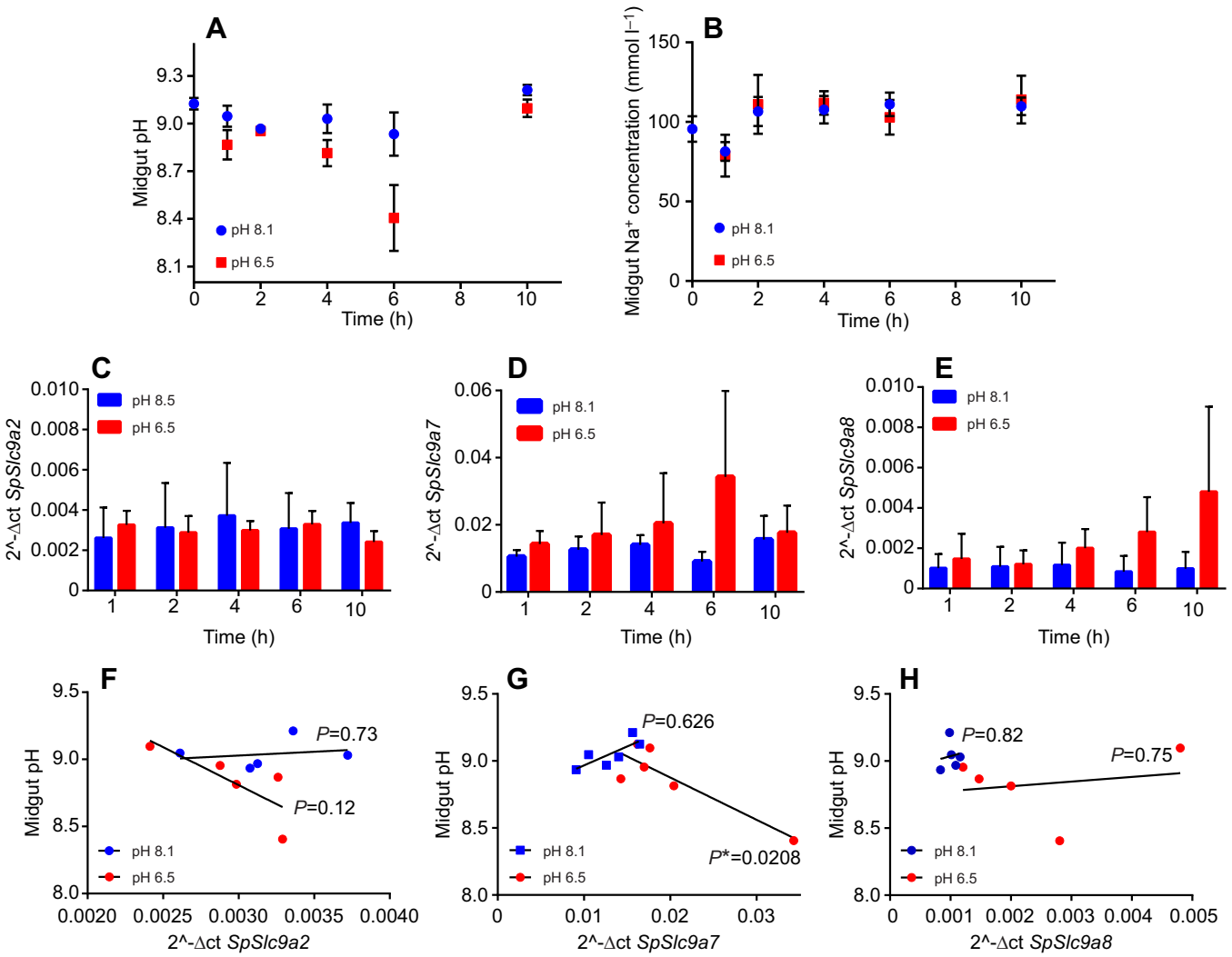

Fig. 5. Midgut pH and [Na^+] and expression of *SpSlc9a2*, *SpSlc9a7* and *SpSlc9a8* during acute exposure to acidified conditions. Measurement of midgut pH (A) and [Na^+] (B) in control (blue) and low pH (red) treated larvae over the 10 h time course. (C–E) Relative expression (2^−ΔCt) of the NHE isoforms *spslc9a2*, *spslc9a7* and *spslc9a8* in control and low pH treated larvae over the 10 h time course. Target genes were normalized to the housekeeping gene *elfa1*. (F–H) Correlation analysis of *spslc9a2*, *spslc9a7* and *spslc9a8* expression in relation to changes in midgut pH (P=0.05). Values are presented as means±s.e.m.; *P<0.05.

localization of SpSlc9a2 leads to the export of Na^+ from the lumen in exchange for H^+. This import of protons into the midgut lumen seems to conflict the alkaline properties of the midgut. However, localization of NHEs in luminal membranes is associated with a range of digestive systems in animals (Zachos et al., 2005; Grosell, 2011; Xu et al., 2018). For example, in the teleost intestine, the putative NHE-2 and NHE-3 are suggested to excrete H^+ into the alkaline intestinal lumen, where HCO_3^- is titrated near the apical surface of the cells to reduce luminal osmotic pressure (Grosell, 2011). In the sea urchin model, this acidified boundary layer may protect midgut epithelial cells from the alkaline digestive conditions. Furthermore, acidification of the intestinal mucosa by NHEs has been demonstrated to be an important feature of H^+-coupled nutrient uptake in mammals (Thwaites et al., 2002; Zachos et al., 2005; Thwaites and Anderson, 2007). For instance, the short-chain fatty acid/OH exchanger in the rat colon as well as the H^+/dipeptide co-transporter are driven by H^+ gradients, which are both functionally linked to brush-border NHE-2 and NHE-3 (Zachos et al., 2005). According to these observations and the results of the present work, it can be concluded that NHE activity in the midgut epithelium of the sea urchin larva contributes to both acid–base and ionic regulation, potentially relevant for digestion and nutrient absorption.

Pharmacological characterization of pH_i regulatory capacities of midgut cells demonstrated that EIPA reduces the speed of the compensation reaction while pH_i is still fully restored. These results suggest that EIPA-sensitive mechanisms are not exclusively responsible for pH_i regulation, underlining the presence of other important acid–base regulatory mechanisms including HCO_3^- transport or VHA activity in midgut epithelial cells of the sea urchin larva. In fact, pH_i regulation in primary mesenchyme cells of the sea urchin larva has been demonstrated to strongly depend on HCO_3^- transport using knockdown and pharmacological approaches (Hu et al., 2018). Furthermore, the sensitivity of luminal alkalization in the sea urchin larva to the V-type H^+-ATPase inhibitor Bafilomycin A1 provides additional pharmacological evidence for the VHA in midgut epithelial cells (Stumpp et al., 2015). As VHA activity has been demonstrated to be involved in pH_i regulatory processes in the Malpighian cells and goblet cells of *Drosophila* larvae and in the tobacco hornworm (Wieczorek et al., 1989, 2009; Bertram and Wessing, 1994) it can be hypothesized that

Journal of Experimental Biology (2021) 224, jeb240705. doi:10.1242/jeb.240705

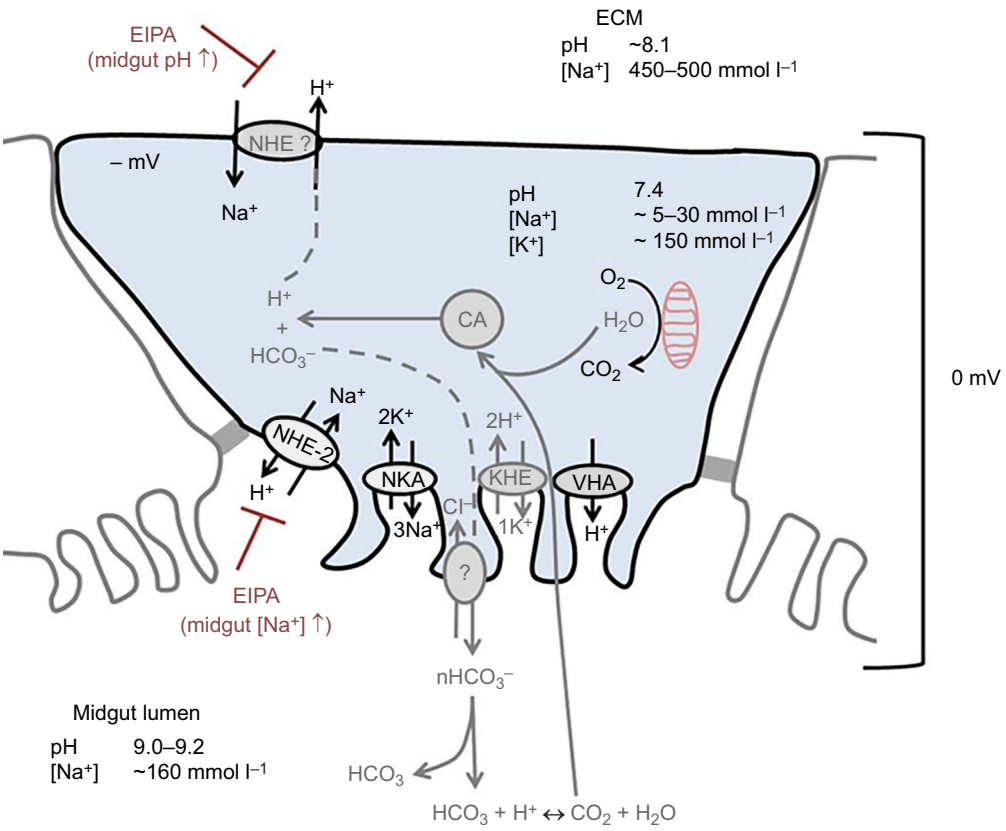

Fig. 6. Putative (grey) and validated (black) transporters and pathways of ion and pH regulation in midgut cells of the sea urchin larva. Pharmacological, immunocytochemical, molecular, as well as midgut pH measurements, confirmed the presence of NHE-2, NKA and the V-type H^+-ATPase in luminal membranes of the midgut epithelium of the sea urchin larva (Stumpp et al., 2015). Hypothetical transporters and pathways that could explain the electroneutral potential of the midgut epithelium are indicated in light grey (Wieczorek et al., 1991; Grosell, 2011; Stumpp et al., 2015). Basolateral application of EIPA reduced midgut alkalization, indicating the presence of Na^+/H^+ exchange mechanisms at the basolateral membrane. Using teleost fish and insects as a guide we hypothesize luminal alkalization by as yet unidentified HCO_3^- transport mechanisms in combination with intracellular carbonic anhydrases. Protons generated by the intracellular CO_2 hydration are removed by basolateral NHEs. H^+ secreted into the lumen can be used to acidify the luminal mucosa to protect cells from the high pH and may contribute to nutrient absorption.

the VHA may also contribute to pH_i regulation in midgut cells of the sea urchin larva. Here, future studies will address a detailed molecular characterization of other pH_i regulatory mechanisms including primary active H^+ transport and the involvement of HCO_3^- transporters in midgut epithelial cells of the sea urchin larva.

Effects of seawater acidification on midgut pH and Na^+ regulation

To identify other Slc9 family members that are potentially involved in regulating the ionic composition of midgut fluids we challenged sea urchin larvae with acidic seawater conditions (pH 6.5). The low pH challenge did not affect midgut [Na^+], indicating that maintenance of luminal pH is not directly linked to transepithelial Na^+ transport rates. In addition, expression levels of *spslc9a2* remained unaffected by the low pH treatment, indicating that this NHE isoform is not involved in defending intracellular or extracellular pH. These findings also corroborate our pharmacological, knockdown and immunohistochemical analyses on the function of SpSlc9a2, which is located in luminal membranes and is mainly responsible for maintaining the luminal Na^+ concentration but not pH. Given the potential role of SpSlc9a2 in mediating boundary layer acidification and nutrient absorption, it is likely that these processes will not be significantly impacted by changes in environmental pH. However, extensive basolateral proton export by other NHE isoforms during more extreme environmental acidification may lead to an increase in intracellular [Na^+] that could then affect Na^+/H^+ exchange in luminal membranes given the relatively low midgut [Na^+]. Thus future studies will use different levels of acute acidification to determine a potential threshold where luminal NHE activity may also be affected.

In contrast to the [Na^+], the pH of midgut fluids was dynamically impacted by the low pH challenge. The biphasic reduction in midgut pH at 1 and 6 h was fully restored both times. The lack of a transcriptional response during the acute compensation of midgut pH at the 1 h time point may be explained by acute post-translational modifications including phosphorylation or translocation of acid–base transporters in midgut epithelial cells. However, during prolonged low pH challenge increased expression of the midgut pH regulatory machinery (i.e. SpSlc9a7 and SpSlc9a8) is used to defend midgut pH. Using a similar approach, the importance of H^+ transporters including NHEs and V-type H^+-ATPases for midgut alkalization has been demonstrated previously (Stumpp et al., 2013). Acute acidification down to pH 7 by addition of CO_2 was accompanied by an initial reduction in midgut pH associated with an upregulation of *NHE-2* (*spslc9a2*) and *VHA* (Stumpp et al., 2013). The contradicting pattern of *spslc9a2* expression may result from the different experimental approaches using CO_2 or HCl to reduce seawater pH. During chronic exposure to environmental hypercapnia *spslc9a2* expression levels were increased (Lee et al., 2019) accompanied by higher feeding rates (Stumpp et al., 2013) to meet the higher energetic demands under acidified conditions. Given the potential role of SpSlc9a2 in supporting nutrient uptake, its upregulation under ocean acidification simulations can be hypothesized to be a consequence of enhanced nutrient absorption rather than acid–base regulation. Finally, infection of pluteus larvae with *Vibrio diazotrophicus* led to an accumulation of bacteria in the gut (Ho et al., 2016; Buckley and Rast, 2019; Stumpp et al., 2020) accompanied by increased *NHE-2* expression (Stumpp et al., 2020). Here it can be also suggested that a large fraction of ingested bacteria is digested and the free nutrients stimulate *NHE-2* expression for the H^+-coupled nutrient uptake.

In this study, two other NHE isoforms, SpSlc9a7 and SpSlc9a8, were stimulated by low pH challenge. Microelectrode measurements demonstrated that midgut pH was restored within 4 h from their lowest pH level (pH 8.4) at the 6 h time point to the 10 h time point

(pH 9.1). This compensation reaction is reflected in the expression level of *spslc9a7*, with highest gene expression detected at the 6 h time point. The expression of *spslc9a8* does not reflect the fluctuation of midgut pH but mRNA levels steadily increase towards the end of the experiments, where midgut pH is largely restored. Even though the cellular localization of these transporters is not known, the increased expression of *spslc9a7* and *spslc9a8* matches the pattern of midgut pH regulation, suggesting a potential link between these NHE isoforms and intra- or extracellular pH regulatory mechanisms in cells of the digestive tract. In mammals, Slc9a7 RNA dot blot analysis of human tissue revealed ubiquitous expression, with most dominant gene expression in regions of the brain, skeletal muscle and secretory tissue, including organs of digestive importance as the stomach, pancreas, small intestine and colon (Numata and Orlowski, 2001). It is suggested that mammalian Slc9a7 is involved in volume regulation of intracellular organelles via K^+/H^+ exchange, but further pharmacological investigation, especially regarding the function of the protein in digestive organs, is needed (Numata and Orlowski, 2001; Kagami et al., 2008; Xu et al., 2018). Slc9a8 mRNA was detected in the apical membrane in fundic and pyloric glands and the brush border of intestinal epithelial cells in mice (Kagami et al., 2008; Xu et al., 2008, 2018). In the mammalian intestine, Slc9a8 was suggested to be involved in sodium absorption from the intestinal brush border of mice and mucosal protection in the gut (Xu et al., 2018). Due to the current lack of histological and functional characterization of SpSlc9a7 and SpSlc9a8 in the sea urchin larva, their contribution to larval midgut pH regulation remains speculative. Thus future studies should be dedicated to a cellular localization and physiological characterization of these NHE isoforms in the sea urchin larva to better understand their potential contribution to acid–base regulatory processes in midgut epithelial cells.

Conclusion

This work presented novel insights into the role of Na^+/H^+ exchange mechanisms in the alkaline midgut of the sea urchin larva. Using pharmacological as well as molecular techniques, different NHEs were identified to contribute to the alkalization process and also to the maintenance of steep [Na^+] gradients between the extracellular space and the larval midgut. While our results provide strong evidence for SpSlc9a2 in regulating midgut [Na^+] and potentially also boundary layer acidification, its exact physiological function of luminal Na^+/H^+ exchange remains speculative. We hypothesized that H^+ ions secreted into the luminal mucosa could be used to protect midgut cells from the highly alkaline digestive environment or may serve H^+-coupled nutrient uptake in the sea urchin larva. However, future studies are needed to address the involvement of SpSlc9a2 in boundary layer acidification and the influence on nutrient uptake.

Determination of intracellular pH regulatory capacities underline an involvement of NHEs in pH_i regulatory abilities of midgut epithelial cells and also highlight the existence of other, as yet unidentified acid–base transport mechanisms. Thus, future studies will test the involvement of HCO_3^- transport pathways by direct injection of inhibitors like acetazolamide or DIDS into the midgut. The potential involvement of HCO_3^- transport in midgut alkalization in combination with Na^+/H^+ exchange mechanisms would highlight conserved alkalization mechanisms in digestive systems of different animal taxa including marine teleosts, insects and echinoderm larvae (Ridgway and Moffett, 1986; Boudko et al., 2001a,b; Corena et al., 2002; del Pilar Corena et al., 2004; Grosell et al., 2005; Grosell, 2011). Here the sea urchin larva can be used as a powerful model to study transmembrane transport mechanisms leading to deeper insights into ionic regulation in a basal deuterostome larva. This knowledge will broaden our understanding of the physiology and diversity of membrane transport systems and will help identify the mechanistic basis for the vulnerability of marine species towards changing environmental conditions.

Acknowledgements

The authors would like to thank M. Stumpp for fruitful discussions on this work. The authors further thank F. Thoben, J. Hildebrand and R. Lingg for maintenance of the sea urchin culture systems.

Competing interests

The authors declare no competing or financial interests.

Author contributions

Conceptualization: I.P., M.Y.H.; Methodology: I.P., M.Y.H., W.W.J.C.; Software: I.P.; Validation: I.P., M.Y.H.; Formal analysis: I.P.; Investigation: I.P., M.Y.H.; Resources: M.Y.H.; Data curation: I.P.; Writing - original draft: I.P.; Writing - review & editing: I.P., M.Y.H., W.W.J.C.; Visualization: I.P., M.Y.H.; Supervision: M.Y.H.; Project administration: M.Y.H.; Funding acquisition: M.Y.H.

Funding

M.Y.H. was funded by the Emmy Noether Program (403529967) of the German Research Foundation (Deutsche Forschungsgemeinschaft).

Data availability

All data used for generating figures and statistical analysis are available in PANGAEA under accession number PDI-26897.

References

Azuma, M., Harvey, W. R. and Wieczorek, H. (1995). Stoichiometry of K^+/H^+ antiport helps to explain extracellular pH 11 in a model epithelium. *FEBS Lett.* **361**, 153-156. doi:10.1016/0014-5793(95)00146-Z

Bachmann, O., Riederer, B., Rossmann, H., Groos, S., Schultheis, P. J., Shull, G. E., Gregor, M., Manns, M. P. and Seidler, U. (2004). The Na^+/H^+ exchanger isoform 2 is the predominant NHE isoform in murine colonic crypts and its lack causes NHE3 upregulation. *Am. J. Physiol. Gastrointest. Liver Physiol.* **287**, G125-G133. doi:10.1152/ajpgi.00332.2003

Bertram, G. and Wessing, A. (1994). Intracellular pH regulation by the plasma membrane V-ATPase in Malpighian tubules of *Drosophila* larvae. *J. Comp. Physiol B* **164**, 238-246. doi:10.1007/BF00354085

Boudko, D. Y., Moroz, L. L., Harvey, W. R. and Linser, P. J. (2001a). Alkalinization by chloride/bicarbonate pathway in larval mosquito midgut. *Proc. Natl. Acad. Sci. USA* **98**, 15354-15359. doi:10.1073/pnas.261253998

Boudko, D. Y., Moroz, L. L., LInser, P. J., Trimarchi, J. R., Smith, P. J. S. and Harvey, W. R. (2001b). *In situ* analysis of pH gradients in mosquito larvae using non-invasive, self-referencing, pH-sensitive microelectrodes. *J. Exp. Biol.* **204**, 691-699.

Brune, A. and Kühl, M. (1996). pH profiles of the extremely alkaline hindguts of soil-feeding termites (Isoptera: Termitidae) determined with microelectrodes. *J. Insect Physiol.* **42**, 1121-1127. doi:10.1016/S0022-1910(96)00036-4

Buckley, K. M. and Rast, J. P. (2019) Immune activity at the gut epithelium in the larval sea urchin. *Cell Tiss. Res.* **377**, 469-474. doi:10.1007/s00441-019-03095-7

Burke, R. D. (1981). Structure of the digestive tract of the pluteus larva of *Dendraster excentricus* (Echinodermata: Echinoida). *Zoomorphology* **98**, 209-225. doi:10.1007/BF00312050

Cameron, R. A., Samanta, M., Yuan, A., He, D. and Davidson, E. (2009). SpBase: the sea urchin genome database and web site. *Nucleic Acids Res.* **37**, D750-D754. doi:10.1093/nar/gkn887

Chintapalli, V. R., Kato, A., Henderson, L., Hirata, T., Woods, D. J., Overend, G., Davies, S. A., Romero, M. F. and Dow, J. A. T. (2015). Transport proteins NHA1 and NHA2 are essential for survival, but have distinct transport modalities. **112**, 11720-11725. doi:10.1073/pnas.1508031112

Clark, T. M., Koch, A. and Mofett, D. F. (1999). The anterior and posterior 'stomach' regions of larval *Aedes aegypti* midgut: regional specialization of ion transport and stimulation by 5-hydroxytryptamine. *J. Exp. Biol.* **202**, 247-252.

del Pilar Corena, M. D. P., Seron, T. J., Lehman, H. K., Ochrietor, J. D., Kohn, A., Tu, C. and Linser, P. J. (2001). Carbonic anhydrase in the midgut of larval *Aedes aegypti*: cloning, localization and inhibition. *J. Exp. Biol.* **205**, 591-602.

del Pilar Corena, M., Fiedler, M. M., VanEkeris, L., Tu, C., Silverman, D. N. and Linser, P. J. (2004). Alkalization of larval mosquito midgut and the role of carbonic anhydrase in different species of mosquitoes. *Comp. Biochem. Physiol. C Toxicol. Pharmacol.* **137**, 207-225. doi:10.1016/j.cca.2003.12.004

Dibrov, P. and Fliegel, L. (1998). Comparative molecular analysis of Na^+/H^+ exchangers: a unified model for Na^+/H^+ antiport? *FEBS Lett.* **424**, 1-5. doi:10.1016/S0014-5793(98)00119-7

Ferguson, D. P., Dangott, L. J. and Lightfoot, J. T. (2014). Lessons learned from vivo-morpholinos: how to avoid vivo-morpholino toxicity. *BioTechniques* **56**, 251-256. doi:10.2144/000114167

Grosell, M. (2011). Intestinal anion exchange in marine teleosts is involved in osmoregulation and contributes to the oceanic inorganic carbon cycle. *Acta Physiol.* **202**, 421-434. doi:10.1111/j.1748-1716.2010.02241.x

Grosell, M., Wood, C. M., Wilson, R. W., Bury, N. R., Hogstrand, C., Rankin, C. and Jensen, F. B. (2005). Bicarbonate secretion plays a role in chloride and water absorption of the European flounder intestine. *Am. J. Physiol. Regul. Integr. Comp. Physiol.* **288**, R936-R946. doi:10.1152/ajpregu.00684.2003

Harkey, M. A. and Whiteley, A. H. (1980). Isolation, culture, and differentiation of echinoid primary mesenchyme cells. *Wilhelm Raux's Arch. Dev. Biol.* **189**, 111-122. doi:10.1007/BF00848500

Heyland, A., Hodin, J. and Bishop, C. (2014). Manipulation of developing juvenile structures in purple sea urchins (*Strongylocentrotus purpuratus*) by morpholino injection into late stage larvae. *PLOS One* **9**, e113866. doi:10.1371/journal.pone.0113866

Ho, E., Buckley, K. M., Schrankel, C. S., Schuh, N. W., Hibino, T., Solek, C. M., Bae, K., Wang, G. and Rast, J. P. (2016). Perturbation of gut bacteria induces a coordinated cellular immune response in the purple sea urchin larva. *Immunol. Cell Biol.* **94**, 861-874. doi:10.1038/icb.2016.51

Hu, M., Tseng, Y.-C., Su, Y.-H., Lein, E., Lee, H.-G., Lee, J.-R., Dupont, S. and Stumpp, M. (2017). Variability in larval gut pH regulation defines sensitivity to ocean acidification in six species of the Ambulacraria superphylum. *Proc. R. Soc. B Biol. Sci.* **284**, 20171066. doi:10.1098/rspb.2017.1066

Hu, M. Y., Petersen, I., Chang, W. W., Blurton, C. and Stumpp, M. (2020). Cellular bicarbonate accumulation and vesicular proton transport promote calcification in the sea urchin larva. *Proc. R. Soc. B Biol. Sci.* **287**, 2-10. doi:10.1098/rspb.2020.1506

Hu, M. Y., Yan, J.-J., Petersen, I., Himmerkus, N., Bleich, M. and Stumpp, M. (2018). A SLC4 family bicarbonate transporter is critical for intracellular pH regulation and biomineralization in sea urchin embryos. *eLife* **7**, e36600. doi:10.7554/eLife.36600

Kagami, T., Kagami, T., Chen, S., Memar, P., Choi, M., Foster, L. J. and Numata, M. (2008). Identification and biochemical characterization of the SLC9A7 interactome. *Mol. Membr. Biol.* **25**, 436-447. doi:10.1080/09687680802263046

Kondapalli, K. C., Todd Alexander, R., Pluznick, J. L. and Rao, R. (2017). NHA2 is expressed in distal nephron and regulated by dietary sodium. *J. Physiol. Biochem.* **73**, 199-205. doi:10.1007/s13105-016-0539-8

Kudtarkar, P. and Cameron, R. A. (2017). Echinobase: an expanding resource for echinoderm genomic information. *Database* **2017**, bax074. doi:10.1093/database/bax074

Lee, H.-G., Stumpp, M., Yan, J.-J., Tseng, Y.-C., Heinzel, S. and Hu, M. Y.-A. (2019). Tipping points of gastric pH regulation and energetics in the sea urchin larva exposed to CO_2-induced seawater acidification. *Comp. Biochem. Physiol. A Mol. Integr. Physiol.* **234**, 87-97. doi:10.1016/j.cbpa.2019.04.018

Luo, Y.-J. and Su, Y.-H. (2012). Opposing nodal and BMP signals regulate left-right asymmetry in the sea urchin larva. *PLoS Biol.* **10**, e1001402. doi:10.1371/journal.pbio.1001402

Morcos, P. A., Li, Y. and Jiang, S. (2008). Vivo-Morpholinos: a non-peptide transporter delivers Morpholinos into a wide array of mouse tissues. *BioTechniques* **45**, 613-614, 616, 618 passim. doi:10.2144/000113005

Numata, M. and Orlowski, J. (2001). Molecular cloning and characterization of a novel $(Na^+,K^+)/H^+$ exchanger localized to the trans-Golgi network. *J. Biol. Chem.* **276**, 17387-17394. doi:10.1074/jbc.M101319200

Okami, T., Yamamoto, A., Omori, K., Takada, T., Uyama, M. and Tashiro, Y. (1990). Immunocytochemical localization of Na^+,K^+-ATPase in rat retinal pigment epithelial cells. *J. Histochem. Cytochem.* **38**, 1267-1275. doi:10.1177/38.9.2167328

Okech, B. A., Boudko, D. Y., Linser, P. J. and Harvey, W. R. (2008). Cationic pathway of pH regulation in larvae of *Anopheles gambiae*. *J. Exp. Biol.* **211**, 957-968. doi:10.1242/jeb.012021

Onken, H., Moffett, S. B. and Moffett, D. F. (2004). The transepithelial voltage of the isolated anterior stomach of mosquito larvae (*Aedes aegypti*): pharmacological characterization of the serotonin-stimulated cells. *J. Exp. Biol.* **207**, 1779-1787. doi:10.1242/jeb.00964

Onken, H., Moffett, S. B. and Moffett, D. F. (2008). Alkalinization in the isolated and perfused anterior midgut of the larval mosquito, *Aedes aegypti*. *J. Insect Sci.* **8**, 46. doi:10.1673/031.008.4601

Patrick, M. L., Aimanova, K., Sanders, H. R. and Gill, S. S. (2006). P-type Na^+/K^+-ATPase and V-type H^+-ATPase expression patterns in the osmoregulatory organs of larval and adult mosquito *Aedes aegypti*. *J. Exp. Biol.* **209**, 4638-4651. doi:10.1242/jeb.02551

Perillo, M., Wang, Y. J., Leach, S. D. and Arnone, M. I. (2016). A pancreatic exocrine-like cell regulatory circuit operating in the upper stomach of the sea urchin *Strongylocentrotus purpuratus* larva. *BMC Evol. Biol.* **16**, 117. doi:10.1186/s12862-016-0686-0

Pullikuth, A. K., Aimanova, K., Kang'ethe, W., Sanders, H. R. and Gill, S. S. (2006). Molecular characterization of sodium/proton exchanger 3 (NHE3) from the yellow fever vector, *Aedes aegypti*. *J. Exp. Biol.* **209**, 3529-3544. doi:10.1242/jeb.02419

Ridgway, R. L. and Moffett, D. F. (1986). Regional differences in the histochemical localization of carbonic anhydrase in the midgut of tobacco hornworm (*Manduca sexta*). *J. Exp. Zool.* **237**, 407-412. doi:10.1002/jez.1402370313

Saier, M. H., , Jr., Eng, B. H., Fard, S., Garg, J., Haggerty, D. A., Hutchinson, W. J., Jack, D. L., Lai, E. C., Liu, H. J., Nusinew, D. P. et al. (1999). Phylogenetic characterization of novel transport protein families revealed by genome analyses. *Biochim. Biophys. Acta Biomembr.* **1422**, 1-56. doi:10.1016/S0304-4157(98)00023-9

Schwenzfeier, A., Wierenga, P. A. and Gruppen, H. (2011). Isolation and characterization of soluble protein from the green microalgae *Tetraselmis* sp. *Bioresour. Technol.* **102**, 9121-9127. doi:10.1016/j.biortech.2011.07.046

Stumpp, M., Hu, M., Casties, I., Sarborowski, R., Bleich, M., Melzner, F. and Dupont, S. (2013). Digestion in sea urchin larvae impaired under ocean acidification. *Nat. Clim. Change* **3**, 1044-1049. doi:10.1038/nclimate2028

Stumpp, M., Hu, M. Y., Melzner, F., Gutowskaa, M. A., Doreyc, N., Himmerkus, N., Holtmann, W. C., Dupontc, S. T., Thorndykec, M. C. and Bleich, M. (2012). Acidified seawater impacts sea urchin larvae pH regulatory systems relevant for calcification. *Proc. Natl. Acad. Sci. USA* **109**, 18192-18197. doi:10.1073/pnas.1209174109

Stumpp, M., Hu, M. Y., Tseng, Y.-C., Guh, Y.-J., Chen, Y.-C., Yu, J.-K., Su, Y.-H. and Hwang, P.-P. (2015). Evolution of extreme stomach pH in bilateria inferred from gastric alkalization mechanisms in basal deuterostomes. *Sci. Rep.* **5**, 10421. doi:10.1038/srep10421

Stumpp, M., Petersen, I., Thoben, F., Yan, J.-J., Leippe, M. and Hu, M. Y. (2020). Alkaline guts contribute to immunity during exposure to acidified seawater in the sea urchin larva. *J. Exp. Biol.* **223**, jeb222844. doi:10.1242/jeb.222844

Thwaites, D. T. and Anderson, C. M. H. (2007). H^+-coupled nutrient, micronutrient and drug transporters in the mammalian small intestine. *Exp. Physiol.* **92**, 603-619. doi:10.1113/expphysiol.2005.029959

Thwaites, D. T., Kennedy, D. J., Raldua, D., Anderson, C. M. H., Mendoza, M. E., Bladen, C. L. and Simmons, N. L. (2002). H^+/dipeptide absorption across the human intestinal epithelium is controlled indirectly via a functional Na^+/H^+exchanger. *Gastroenterology* **122**, 1322-1333. doi:10.1053/gast.2002.32992

Wieczorek, H., Beyenbach, K. W., Huss, M. and Vitavska, O. (2009). Vacuolar-type proton pumps in insect epithelia. *J. Exp. Biol.* **212**, 1611-1619. doi:10.1242/jeb.030007

Wieczorek, H., Putzenlechner, M., Zeiske, W. and Klein, U. (1991). A vacuolar-type proton pump energizes K^+/H^+ antiport in an animal plasma membrane. *J. Biol. Chem.* **266**, 15340-15347. doi:10.1016/S0021-9258(18)98621-7

Wieczorek, H., Weerth, S., Schindlbeck, M. and Klein, U. (1989). A vacuolar-type proton pump in a vesicle fraction enriched with potassium transporting plasma membranes from tobacco hornworm midgut. *J. Biol. Chem.* **264**, 11143-11148. doi:10.1016/S0021-9258(18)60441-7

Xu, H., Chen, H., Dong, J., Lynch, R. and Ghishan, F. K. (2008). Gastrointestinal distribution and kinetic characterization of the sodium-hydrogen exchanger isoform 8 (NHE8). *Cell. Physiol. Biochem.* **21**, 109-116. doi:10.1159/000113752

Xu, H., Ghishan, F. K. and Kiela, P. R. (2018). SLC9 gene family: function, expression, and regulation. *Compr Physiol.* **8**, 555-583. doi:10.1002/cphy.c170027

Zachos, N. C., Tse, M. and Donowitz, M. (2005). Molecular physiology of intestinal Na^+/H^+ exchange. *Annu. Rev. Physiol.* **67**, 411-443. doi:10.1146/annurev.physiol.67.031103.153004